Supporting information to "The Electron Depolarization in Dynamic Nuclear Polarization: Measurements and Simulations"

S1. Analysis of the ELDOR data of the TEMPOL using the TM formalism

In section 4 of the main text we considered the formation of spin temperature in our samples. The E_{excite} profiles detected at 7 K in Fig. 4a show only very little dependence on $\delta\nu_{detect}$, which could then be interpreted by introducing a very large T_{enZ} values. This spin temperature should be equal to the nuclear Zeeman temperature, $T_{nz} = T_{enZ}$, according to the TM-DNP description [18, 19], resulting in nuclear polarization of

$$P_n = \tanh\left(\frac{\omega_n \hbar}{2k_B T_{enZ}}\right). \tag{24}$$

Realizing that the ELDOR frequency profiles change only slightly for t_{excite} values close to the DNP timescale, large T_{enZ} values should result in a very low nuclear enhancement. This prediction should then be consistent with the maximum DNP enhancement, $|\epsilon_{DNP}| = |P_n(t)/P_n(0)|$, that was measured by Shimon *et al.* [44] at 6 K on a similar sample and with the same experimental setup, as given in their supplementary information. During their DNP experiments they obtained an enhancement of about 60, which results in a value for $|T_{nZ}|$ which is about 0.12 K according to

$$|\epsilon_{DNP}| = |\frac{\tanh(\omega_n \hbar/2k_B T_{nZ})}{\tanh(\omega_n \hbar/2k_B T_L)}|, \tag{25}$$

and thus much smaller than the sample temperature. This result is inconsistent with the high T_{enZ} value derived from the ELDOR data, showing that we can nor use the TM-DNP formalism to describe the enhancement process.

Another example, showing that the electron polarizations cannot be described by a spin temperature, can be given by again using the enhancements measured by Shimon *et al.* [44]. They obtained enhancements of aboutϵ_{DNP} =60 and -55 when irradiating at $\delta\nu_{excite} = -150$

MHz and 100 MHz, respectively. As derived above, the corresponding $T_{nZ} = T_{enZ}$ spin temperatures at these $\delta\nu_{excite}$ frequencies are about 0.14 K or less. Using this value for T_{neZ}, the change in the electron polarization detected at $\delta\nu_{detect} = -150$ MHz and $\delta\nu_{detect} = 100$ MHz should result in a change of about $|\tanh(\frac{2\pi\cdot 250\times 10^6\hbar}{2k_B T_{neZ}})/\tanh(\frac{\omega_e\hbar}{2k_B T_L}) \simeq 14\%$ in the detected normalized polarizations, and with a opposite slope for the two excitation frequencies. Such changes were clearly not detected.

S2. Electron hyper- and hypo- polarizations induced by hyperfine and dipolar interactions.

In this SI we consider the electron polarization in small model spin systems in an effort to find possible sources of the experimentally detected electron hyperpolarization and depolarization observed in the ELDOR data of the trityl sample at 30 K. These features show up during MW irradiation at frequencies close to the edges of the EPR line. In addition we will try to address the polarization transfer between electron packets separated in frequency that lead to the local minima in the E_{detect} spectra observed in this sample at 2.7 K. Here we show that these features can appear when strong hyperfine or electron-electron dipolar interactions are present causing large line splittings in the SQ spectra of the electrons.

The ELDOR profiles of the model systems shown here were generated using the QM based simulations, described in Refs. [21, 25], using the parameters given in Table S.1. During these calculations the temporal evolution of the spin density matrix, $\rho(t)$, is evaluated in the presence of all relevant interactions, relaxation parameters and MW irradiation. Frequency selective EPR echo detection is assumed during signal analysis[78]. At the first stage the thermal equilibrium density matrix ρ_0 is propagated during a MW irradiation at a frequency ν_{excite} and of a duration t_{excite}, resulting in $\rho(\nu_{excite}, t_{excite})$. Next, a weak selective $(\pi/2)_x$ pulse at a frequency of ν_{detect} is applied on the system, resulting in $\rho^+(\nu_{excite}, t_{excite}, \nu_{detect})$, and the signal in the y direction is calculated using $S_e(\nu_{excite}, t_{excite}, \nu_{detect}) = Tr(S_y\rho^+(\nu_{excite}, t_{excite}, \nu_{detect}))$, where S_y is the electron spin operator in the y direction. This value can be normalized with respect to the electron thermal polarization, as given by $P_{e,0} = Tr(S_z\rho_0)$.

For the first model spin system we consider a single electron that is strongly hyperfine coupled to a ^{13}C nucleus and that exhibits an EPR spectrum consisting of a large isotropic hyperfine split doublet of lines. A small pseudo-secular $A^{\pm}$ hyperfine interaction term is added to allow for a polarization transfer between the electron and the nucleus *via* the SE mechanism. This two-spin system resembles in some way the strong intramolecular interactions between a natural abundance^{13}C nucleus and the unpaired electron in trityl [66].

In Fig. S.1 we show steady state $S_e(\nu_{excite})$ spectra, with the electron polarizations detected at $\nu_{detect} = \nu_e - \frac{1}{2}A_z$ (black) and $\nu_{detect} = \nu_e + \frac{1}{2}A_z$ (blue), where $A_z = 20$ MHz is the strength of the isotropic hyperfine interaction. When $T_{1n} \gg T_{1e}$ and at 30 K (solid lines in S.1a) the saturation at $\nu_{detect} = \nu_e \pm \frac{1}{2}A_z$ reaches zero when $\nu_{excite} = \nu_{detect}$, shows a depolarization when $\nu_{excite} = \nu_e \pm \nu_{^{13}C}$, and a hyperpolarization when $\nu_{excite} = \nu_e \mp \nu_{^{13}C}$, respectively. This resembles the trends of the hyper- and de- polarization features observed experimentally at 30 K. The amounts of enhanced and depleted saturation depend on the steady state nuclear polarization, which is limited by the thermal value of the electron polarization. We therefore expect these amounts to increase when lowering the temperature, as can be seen in Fig. S.1b (solid lines), where the simulation temperature was chosen to be 2.7 K. These results differ dramatically form the experimental ones, where mainly depolarization of the electrons is seen. In order for the simulated polarization profiles to result in large depolarizations it is necessary to consider a fast cross-relaxation mechanism in the electron-nucleus system, which for simplicity can be introduced by decreasing T_{1n}. When choosing a T_{1n} value close to T_{1e} in the simulations the saturation spectra shows strong depletion of the enhancement when irradiating at $\nu_{excite} = \nu_e \pm \frac{1}{2}A_z$ or $\nu_e \pm \nu_{^{13}C}$, as plotted in Fig. S.1b (dashed lines). Such a mechanism can explain the experimental E_{detect} spectra, where depolarization of the electron polarization is observed when irradiating far away from the detected electrons, and which cannot be attributed to the eSD mechanism.

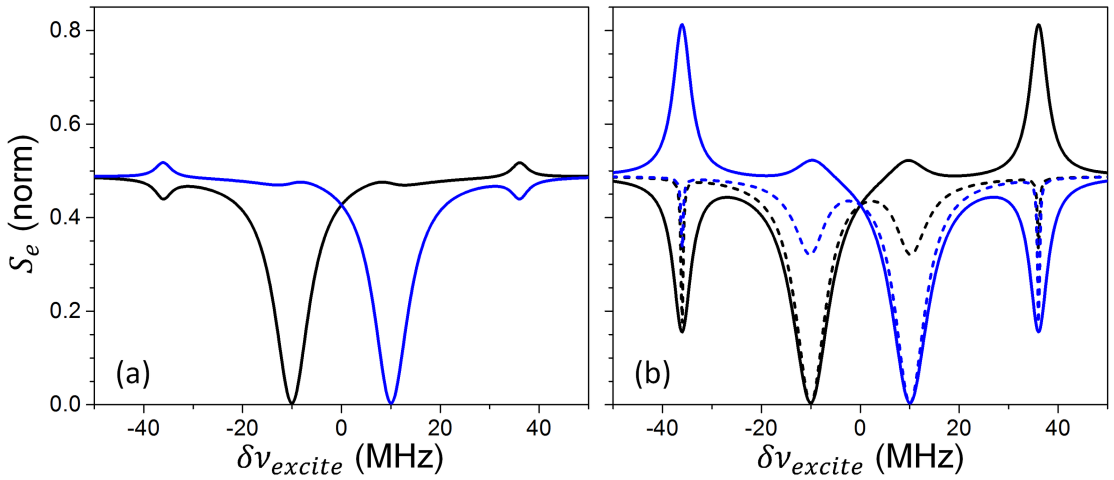

Figure S.1: Simulated steady state S_e as a function of $\delta\nu_{excite} = \nu_{excite} - \nu_e$ in an electron-nucleus two spin model. The detection was performed at $\nu_{detect} - \nu_e = -10$ MHz (black) or 10 MHz (blue). A temperature of 30 K was used in (a), and 2.7 K in (b). T_{1n} of 1s (solid lines) or 3.2 ms (dashed lines) were used, with the latter corresponding to the value of T_{1e}. All other parameters were taken from Table S.1, and the results are normalized with respect to $P_{e,0}$ at the corresponding temperature.

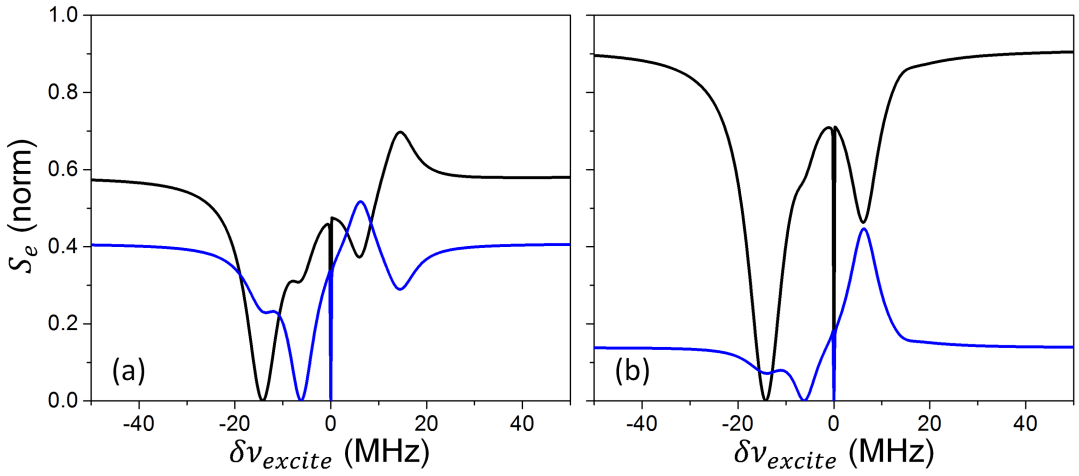

Figure S.2: Simulated steady state S_e as a function of $\delta\nu_{excite} = \nu_{excite} - \nu_{e,0}$ in an electron-electron two spin model. The detection was performed at $\nu_{detect} - \nu_{e,0} = -14.2$ MHz (black) or -6.2 MHz (blue), which corresponds to the main transitions of one of the electrons. A temperature of 30 K was used in (a), and 2.7 K in (b). All other parameters were taken from Table S.1, and the results are normalized with respect to $P_{e,0}$ at the corresponding temperature.

The second small spin system consists of two strong dipolar interacting electrons, $e_a - e_b$. This can be correlated to a randomly oriented close electron pair in the sample, or to a dimer of radicals. The four electron transitions in this system are positioned at about $\nu_{e,0} \pm \delta\nu_{ab} \pm D$, where D is the dipolar interaction between the electrons and $\nu_{e,0} \pm \delta\nu_{ab}$ are the resonance frequencies of the electrons. In Fig. S.2 we show simulated steady state $S_e(\nu_{excite})$ spectra for a system with EPR lines at ± 14.2 and ± 6.2 MHz removed from $\nu_{e,0}$ and with ν_{detect} equal to $\nu_{e,0} - 14.2$ MHz or $\nu_{e,0} - 6.2$ MHz. The $S_e(\nu_{excite})$ spectra for ν_{detect} equal to $\nu_{e,0} + 14.2$ MHz or $\nu_{e,0} + 6.2$ MHz are very similar but with an opposite sign of the features with respect to $\nu_{e,0}$.

Starting from 30 K (Fig. S.2a) it can be seen that an irradiation on each of the electron transitions results in a hyperpolarization or depolarization. In addition we observe a narrow depletion when $\nu_{excite} = \nu_{e,0}$. This is due to electron DQ transitions, which are not expected to play an important role in more complex systems. When performing the simulation using 2.7 K (Fig. S.2b) some of the EPR line intensities are stronger than others due to the Boltzmann distribution, and in particular the outer transitions show stronger intensities than the two inner ones. The resulting profiles again show both hyper- and hypo- polarization features, however they differ from those at 30 K due to the change in the Boltzmann distribution. The magnitudes of these effects change when changing the state mixing in the system, depending on the $|D/\delta\nu_{ab}|$ ratio, however in general electron hyperpolarization and

depolarization effects appear in all spectra. To combine these modulations of the polarization with randomly oriented electron pairs, with a distribution of $\delta\nu_{ab}$ and D values, while taking into account the spectral diffusion mechanism, is not straightforward and it is therefore hard to predict whether this will result in the experimentally detected features observed at 2.7 K.

To conclude, the above model systems offer a way by which electron hyperpolarization and depolarization can be achieved at frequencies removed from the detected frequency. Since we can expect that large hyperfine or dipolar split transitions will have a larger relative weight at the side of the EPR line when compared with electrons with small interactions, such effects will be more dominant when detecting far from the center of the EPR line, as was seen experimentally.

Parameter	value
$\omega_1/2\pi$ [MHz]	0.6
$\omega_{1,detect}/2\pi$ [MHz]	0.1
T_{1e} [ms]	5
T_2 [μs]	100
T_{1n} [s]	1
$A^{\pm}$ [MHz]	4
A_Z [MHz]	20
D [MHz]	4
$\delta\nu_{ab}$ [MHz]	20

Table S.1: Parameters used in the simulations of small model spin systems.